

Measurement of the Two-Photon Decay of the K_L^0 Meson*

J. Enstrom, G. Akavia,† R. Coombes, D. Dorfan,‡ D. Fryberger, R. Piccioni, D. Porat, D. Raymond,§
 K. Riley,|| A. Rothenberg, H. Saal, M. Schwartz, and S. Wojcicki**
Stanford Linear Accelerator Center, Stanford University, Stanford, California 94305
and Physics Department, Stanford University, Stanford, California 94305
 (Received 2 June 1971)

A measurement of the rate $\Gamma(K_L^0 \rightarrow 2\gamma)$ has been made relative to the rates $\Gamma(K_L^0 \rightarrow 3\pi^0)$, $\Gamma(K_L^0 \rightarrow \pi^+\mu^-\nu_\mu)$, and $\Gamma(K_L^0 \rightarrow \pi^+e^-\nu_e)$ in a spark-chamber scintillation-counter experiment. Using published branching ratios of the three-body decays relative to the rate $\Gamma(K_L^0 \rightarrow \text{all})$, the branching ratio $\Gamma(K_L^0 \rightarrow 2\gamma)/\Gamma(K_L^0 \rightarrow \text{all})$ has been found to be $(4.5 \pm 1.0) \times 10^{-4}$, based on 23 valid decays, which were separated from a small background.

I. INTRODUCTION

We report herewith on an experimental determination of the two-photon decay rate of the long-lived neutral kaon (K_L^0) relative to its total decay rate. Specifically we find

$$\frac{\Gamma(K_L^0 \rightarrow 2\gamma)}{\Gamma(K_L^0 \rightarrow \text{all})} = (4.5 \pm 1.0) \times 10^{-4}.$$

This result is in good agreement with previous experiments¹⁻⁶ and with crude model-dependent theoretical predictions.^{1-3,7-18} In one of these models,¹ for example, the 2γ decay is taken to proceed through an intermediate state of either π^0 or η^0 with the relative amplitude of these two states given by SU(3). We would then have a matrix element for the decay of K_L^0 into 2γ given by

$$M(K_L^0 \rightarrow 2\gamma) = f_{K\pi} \left(\frac{m_K^2}{m_K^2 - m_\pi^2} \right) M(\pi^0 \rightarrow 2\gamma) \\ + f_{K\eta} \left(\frac{m_K^2}{m_K^2 - m_\eta^2} \right) M(\eta^0 \rightarrow 2\gamma),$$

where SU(3) would yield the relation $f_{K\eta} = (\frac{1}{3})^{1/2} f_{K\pi}$. The corresponding rates would then become

$$\frac{\Gamma(\eta^0 \rightarrow 2\gamma)}{\Gamma(\pi^0 \rightarrow 2\gamma)} = \left| \frac{M(\eta^0 \rightarrow 2\gamma)}{M(\pi^0 \rightarrow 2\gamma)} \right|^2 \frac{m_\eta^3}{m_\pi^3}$$

and $\Gamma(K_L^0 \rightarrow 2\gamma) = (4.3 \pm 1.9) \times 10^{18} f_{K\pi}^2$. The error in the above prediction arises from the measurement error in the determinations of the π^0 and η^0 decay rates.¹⁹ Various estimates^{2,13,15} of the constant $f_{K\pi}$ have been made. If one uses the hypothesis of partially conserved axial-vector current (PCAC) one might anticipate a value for $f_{K\pi}$ in the range of 10^{-5} to 10^{-4} leading to a prediction of

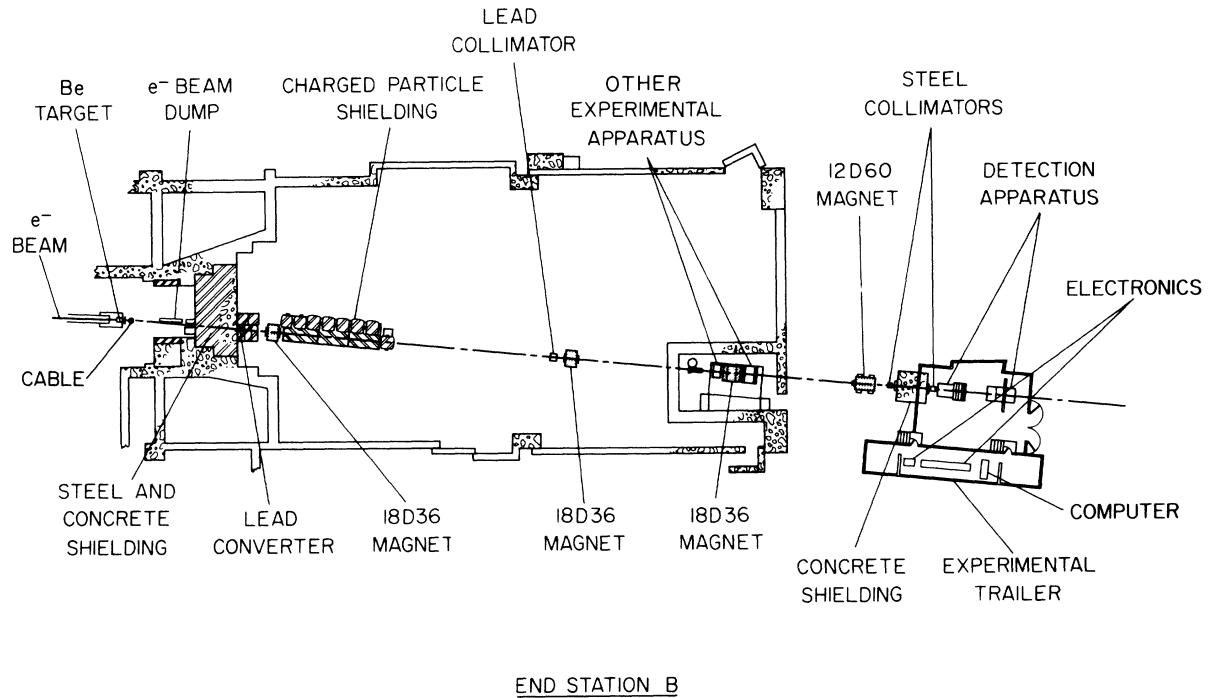
$$\left[\frac{\Gamma(K_L^0 \rightarrow 2\gamma)}{\Gamma(K_L^0 \rightarrow \text{all})} \right]_{\text{predicted}} \sim 10^{-4} \text{ to } 10^{-3}.$$

II. EXPERIMENTAL PROCEDURE

The experiment was carried out at the Stanford Linear Accelerator Center²⁰ by observing the decays of K_L^0 in a large spark chamber and scintillation-counter array. These kaons were produced in a beryllium target at 3° to the incident electron beam (see Fig. 1) and were allowed to pass through a succession of sweeping magnets before entering our experimental apparatus. The total flight path from target to detector was 80 m.

An important characteristic of the 16-GeV electron beam that was used to produce our kaons was its time structure.²⁰ A beam "knockout" system was used to eliminate all but one rf bunch every 50 nsec. Within each rf bunch the electrons were limited to about 10° in phase leading to an inherent bunch length of 1/100 nsec at the target. Thirty such bunches comprised one 1.5- μ sec pulse of the machine; we normally accepted 180 pulses/sec on the target. The reason for requiring this time structure was the desire to measure the energy of each K_L^0 involved in a decay by determining its time of flight with high accuracy. Ultimately, the energy resolution corresponded to an over-all timing accuracy of $\pm \frac{1}{2}$ nsec out of 250 nsec and was limited only by the resolution of one large counter.

The spectrum of kaons produced at the target has been established by Leith and collaborators in an independent bubble-chamber experiment²¹ and is shown in Fig. 2. The beam produced at the target was passed through a 12-in.-thick lead converter for removing the γ -ray contamination. It was next passed through a succession of sweeping magnets, collimators, and shielding tunnels to remove both primary and secondary charged particles and to provide spatial definition. It finally entered the experimental apparatus illustrated in Fig. 3. As the beam entered the detector it consisted about equally of kaons and neutrons, most of the latter being below 1 GeV/c in momentum

FIG. 1. K_L^0 beam line.

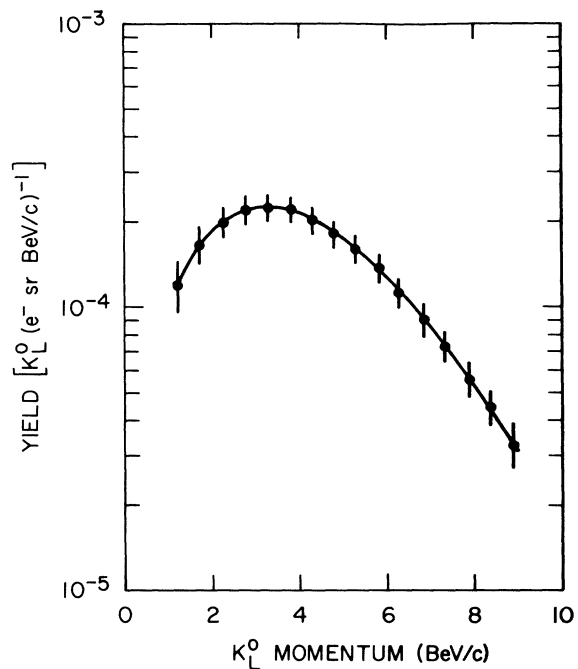
and arriving quite late. The neutrons did not constitute a meaningful background for this experiment.

The beam passed into the detection region through a final collimator which was sufficiently large so no kaons which had been undeflected by the earlier collimators could have struck its walls. The beam then entered the decay region itself.

Two separate groups of data were taken during the course of the experiment. During the first data run the beam was collimated to a height of 1 in. and a width of 5 in. During the second data run the particles were collimated into two separate 1×1 -in. beams separated by a horizontal distance of 6 in. The high level of collimation was necessitated by the desire to set a firm spatial constraint on the origin of the decay products when reconstructing our events.

The decay volume itself was surrounded by a four-sided aluminum frame box with a 47-in. \times 47-in. internal cross section and 48-in. length. The inside of the box was lined with a $\frac{1}{2}$ -in.-thick layer of lead. Within the lead box was a helium bag to reduce the probability of kaon interactions. Each of the four sides on the outside of the box was covered by three pairs of $\frac{1}{2} \times 12 \times 60$ -in. scintillation counters with $\frac{1}{2}$ in. of Pb between the two counters of each pair. There were two additional counters placed on the top and bottom sides of the box to

make a total of 26 counters, which we call L counters. The downstream vertical end of the box was covered with four $\frac{1}{2} \times 11 \times 60$ -in. scintillation coun-

FIG. 2. K_L^0 momentum spectrum at target.

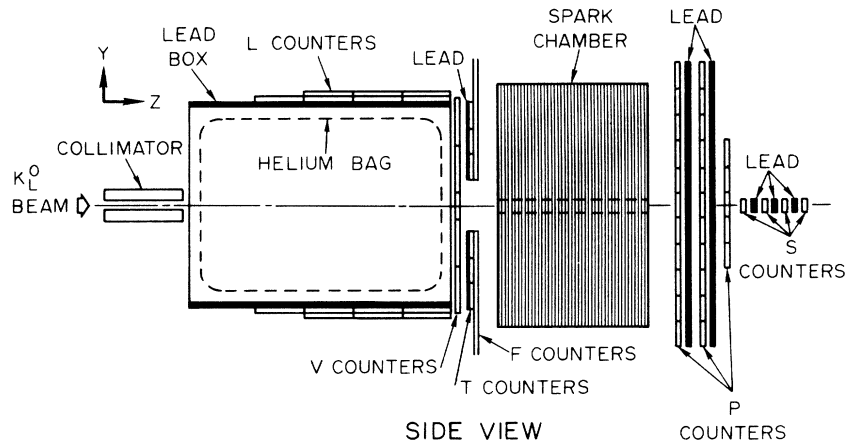


FIG. 3. Detection apparatus (collimation for first data run).

ters, two above beam level and two below beam level, and two $\frac{1}{2} \times 6 \times 33$ -in. counters at beam level. These were known as *V* counters and were arranged as shown in Fig. 3. The lead box and *L* counters were used to convert and detect the presence of photons, which originated from the neutral decay modes of kaon and did not enter the spark chamber. They did not participate in the logic used to trigger the chambers themselves. The *V* counters were used to detect the presence of charged particles which occurred in the charged decay modes.

Downstream of the *V* counters were two $\frac{1}{4} \times 18 \times 60$ -in. slabs of lead, each displaced 6 in. vertically from the center-of-the-beam line, which acted as converters for photons which came from the neutral kaon decays. Immediately downstream of the lead was the bank of counters called *T* counters, consisting of three horizontal counters above and three below the beam, again displaced 6 in. from the center of the beam. Each of these counters was $\frac{1}{2} \times 6 \times 60$ in. and was equipped with a photomultiplier tube at each of its ends. In a plane immediately downstream of the *T* counters were 16 vertical counters, called *F* counters, eight be-

low the beam and eight above the beam. These *T* and *F* counters were used to determine accurately the time of flight of the kaons.

The spark chamber located just downstream of the *T* and *F* counters was of somewhat unconventional design. The 21 ground plates were made of $\frac{1}{2}$ -in.-thick aluminum, each 63×63 in. in area. The 20 high-voltage plates, on the other hand, were made of $\frac{1}{2}$ -in. copper-clad Fiberglas-epoxy. This was done to enable each high-voltage plane to be subdivided electrically into two independent parts; in this way the over-all multitrack efficiency of the chamber was enhanced considerably. A 9×2 -in. hole through the chamber permitted the passage of the residual beam with minimal interaction.

Following the spark chamber were two full banks of 22 horizontal counters, called *P* counters, which absorbed the showers originating in the spark chamber. They were separated by a $\frac{1}{2}$ -in.-thick slab of lead converter. The counter-lead-counter sandwich was followed by a second slab of lead and a partial bank of ten more counters, centered about the beam line. The *P* counters were each $\frac{1}{2} \times 6 \times 33$ in. The output current from the

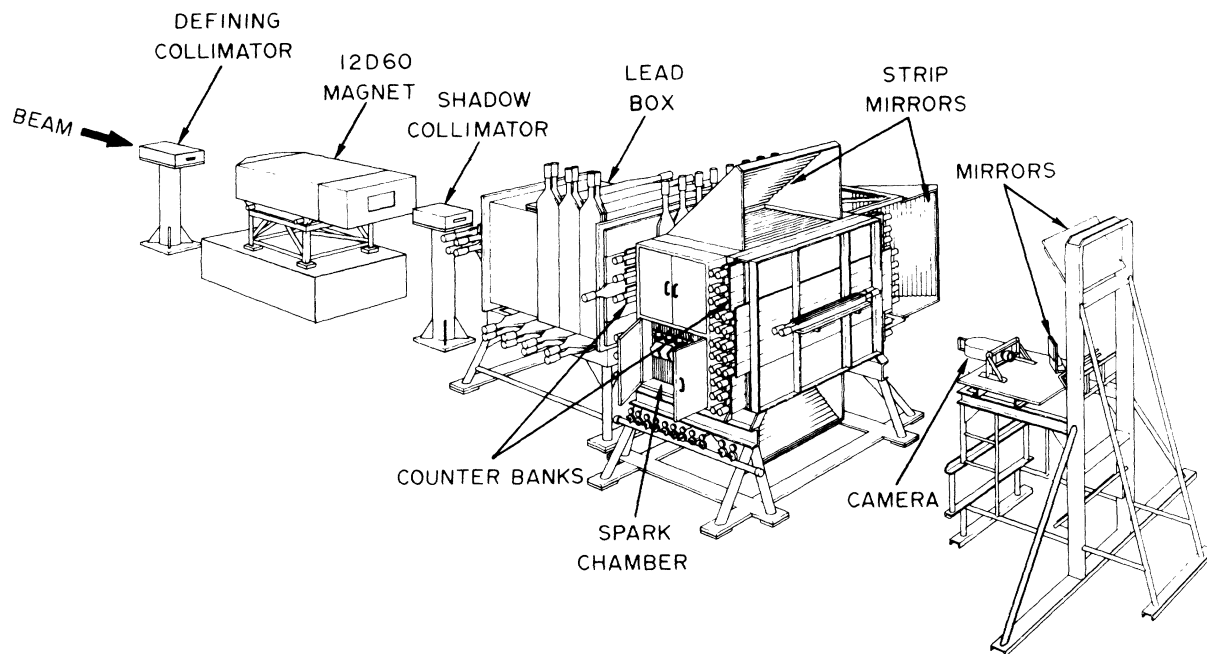


FIG. 4. Perspective view of detection apparatus (collimation for second data run).

photomultiplier tubes for counters in the same vertical position in each of the three banks was summed directly to obtain a combined pulse, which was roughly proportional to the total energy deposited in those counters. Following the P counters were four small $\frac{1}{4} \times 2 \times 18$ -in. counters, with each of the last three preceded by a $\frac{1}{4}$ -in.-thick piece of lead. These were called S counters and were used to convert and detect any γ 's which had gone through the hole in the chamber and P -counter lead. The arrangement of the P and S counters is shown in Fig. 3.

Photographs containing a top, bottom, and side view of the spark-chamber gaps were taken of each event using a mirror system which focused the light on the camera lens. A perspective-view sketch of all the apparatus as it was actually set up for the second data run is shown in Fig. 4. The concrete wall following the shadow collimator has been removed from the sketch for clarity.

A PDP-9 computer was used for the on-line storage, histogramming, and displaying of data taken during the operation of the experiment.²² All of the pulse height and timing signals from the various counters, along with identification information, were recorded on tape for each event. Various electronic modules were used to standardize the pulses received from the computers and to form logic circuits which triggered the apparatus. An important role was played by a set of accurate fast analog to digital converters (ADC) designed for this experiment²³ and used to determine the

times and heights of all T and F pulses and the pulse heights in the P counters.

Whenever the requirements for triggering an event were satisfied the spark chamber was fired. A gating pulse from the event trigger was sent to the ADC modules which enabled them to accept and start processing the pulse height and timing data from the counters. The triggering logic was then disabled and the digital data in the ADC modules was transferred into the computer. The film was advanced to the next frame and the background lights, fiducial lights, and roll-frame number were flashed on. The event logic was again enabled and made ready to accept the next event. There were basically two triggers used in the data taking: The neutral-event trigger, and the charged-decay trigger referred to as the monitor trigger. The monitor trigger was used once after every 10 neutral events to obtain an independent sample of kaon-decay events, and whenever it was used a special light was registered on the film.

The neutral-event trigger was used to obtain samples of the neutral decay modes of the K_L^0 , namely, 2γ , $2\pi^0$, and $3\pi^0$. Data on all of these modes were taken with a similar trigger requirement which included the following.

1. No count must be present in the V counter.
2. Simultaneous pulses must be observed from each end of at least one T counter.
3. A pulse from at least one F counter consistent with the struck T counter must be observed.
4. A pulse from at least one counter in each of

two subsets of the set of P counters must be observed. (The two subsets were arrayed like the squares on a checkerboard.) This requirement was satisfied by nearly all showers which naturally spread out to encompass neighboring P counters. It was not satisfied by many of the single background pions and muons.

5. A timing pulse ("cable") obtained by passing the primary electron beam through a coaxial cable at the target must be observed. This timing pulse was exceedingly sharp ($\sim \frac{1}{10}$ nsec at the detector) and provided a reference for all of the ADC modules used as timing circuits.

The monitor-event trigger was used to observe a sample of the charged decay modes of the K_L^0 , namely, $\pi\mu\nu_\mu$, $\pi e\nu_e$, and $\pi^+\pi^-\pi^0$. Two variations of this trigger were used during the data taking. In the early part of the run the requirement consisted of pulses from one upper V counter, one lower V counter, and one valid T - F coincidence, along with a cable pulse. In the latter part of the run another pair of V counters was added between the earlier four in order to increase the triggering probability and a pair of counters (B) was placed about the beam upstream of the decay volume to serve as a collimator. This trigger required that no B counters and any two of the three V -counter pairs had to fire.

Routine monitoring and calibration of the timing system were carried out in two ways. Light pulsers situated on each counter were activated regularly and their timing recorded to calibrate the system internally. Calibration relative to the electron beam was accomplished by turning off the magnets and allowing muons produced at the target to pass into the system. A study of the self-consistency of the T and F counters on individual muons yielded a value for the over-all timing accuracy of $\pm \frac{1}{2}$ nsec.

III. DATA REDUCTION AND ANALYSIS

Approximately 200 000 pictures were used in the analysis. A scanning of all film by physicists served to separate the events of interest from background and to classify them. The background ($\sim 70\%$ of the pictures taken) were largely blanks or kaon interactions in the chamber.

Valid neutral kaon decays were classified by the number of visible showers (two to six) observed in the chamber. Monitor events were classified according to the decay mode wherever possible. The triggering efficiency for the $\pi^+\pi^-\pi^0$ decay mode on a monitor trigger was small and all residual candidates for this decay mode were excluded from further consideration.

The scanned events of interest were then mea-

sured on an image-plane digitizer. The digitizer measured in two dimensions on the table with a resolution which corresponded to 1 count per 0.01 in. in real space. In measuring the γ tracks, the direction was determined from the first several sparks and the central core of the resulting shower, and the range was determined by the distance between the first and last sparks. In measuring the charged tracks, the direction was determined by the sparks from the initially unscattered portion of the track.

Using the digitized data for the spark coordinates of each measured event the tracks were reconstructed into a three-dimensional coordinate system and the direction cosines of each of the γ rays was obtained by a least-squares method. These preliminary fits on the individual tracks were then combined to obtain a best fit for a common vertex subject to the constraint that it lie in the collimated decay region.

All times as read by our ADC modules were then corrected by subtracting from them the reference time required for a particle traveling with the velocity of light to traverse the distance from the beginning of the target to the trigger-counter bank. (This reference time was obtained by means of muons as mentioned earlier.) By knowing which F and T counters were struck we were able to correct all measured times to a common kaon flight time, taking into account the velocity of propagation of light in the scintillator as well as the time taken by a decay product in traveling from the vertex to the counter. A final correction was made for the time slewing which is associated with phototube pulse-height variation. The time-of-flight distribution obtained in this way is shown in Fig. 5.

In order to determine the branching ratio of interest we must normalize to the total number of decays which occur within our decay region. Two independent determinations of this normalization

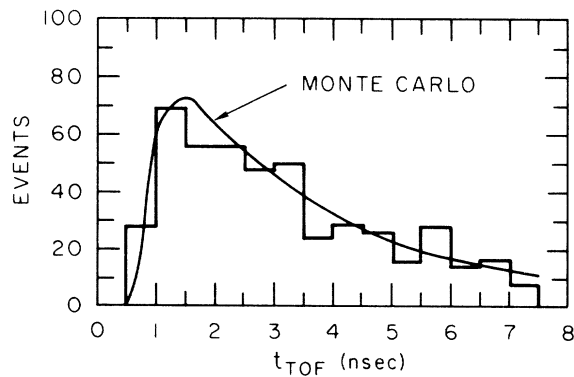


FIG. 5. K_L^0 time-of-flight distribution for good 3-6 γ events from second data run.

have been made, one based on the observed number of $3\pi^0$ events and the other based on the observed rate of $\pi e\nu$ and $\pi\mu\nu$ decays. In each case a Monte Carlo calculation served to relate the observed number of decays coming from a given region to the total number of decays in that region.

We consider first the $3\pi^0$ normalization. The two important parameters which enter into the Monte Carlo calculation are the γ -ray conversion probability in the lead preceding the trigger counters and the γ -ray conversion probability in the spark chamber itself. These quantities were estimated from known absorption cross sections and were then checked experimentally by studying the actual decays themselves. The absorption cross sections used were

$$\mu_{Pb} = 0.112 \text{ cm}^2/\text{g},$$

$$\mu_{Al} = 0.029 \text{ cm}^2/\text{g},$$

$$\mu_{\text{Fiberglass-epoxy}} = 0.027 \text{ cm}^2/\text{g}.$$

These numbers yielded an over-all conversion probability in the lead or the $\frac{1}{2}$ -in. counter immediately following it of 0.55. The conversion probability in the spark chamber was equal to 0.96.

The trigger efficiency was checked experimentally by counting the number of times a γ ray from a 6γ event traversed but failed to convert in the lead. The distribution of conversion points in the chamber served to check the conversion probability in the plates. Both of the above measurements were in good agreement with expectations.

A Monte Carlo program was also used to simulate the leptonic decays, $K_L^0 \rightarrow \pi\mu\nu_\mu$ and $K_L^0 \rightarrow \pi e\nu_e$, following the same procedure as with the neutral events, and using well-known decay distributions and parameters.^{19,24}

For purposes of more accurate reconstruction, we limited the sample of measured monitor events to those where the pion did not interact before the fifth gap, which meant that the pion had to penetrate two aluminum plates and two Fiberglass-epoxy plates, corresponding to 11.5 g/cm^2 of material. If the pion also went through the $\frac{1}{4}$ in. of lead and the three $\frac{1}{2}$ -in.-thick layers of T counters, support wood, and F counters, this represented an additional 11.1 g/cm^2 of material. The interaction length of pions in aluminum is 80 g/cm^2 and in lead is 160 g/cm^2 . For the muonic decays, we required that the muon had to be energetic enough to travel through the lead and trigger counters and the entire spark chamber, which corresponded to a range of about 125 g/cm^2 and a muon energy of at least 0.35 GeV . For the electronic decays, we required that the electron not hit the lead. These requirements which we used

in selecting the measured events were also used in the Monte Carlo program, so that we obtained the triggering efficiency for the same class of events which we actually measured. We obtained an average efficiency by integrating over the same momentum range and decay-point range as was used for the neutral decays.

The total number of K_L^0 decays as derived from the three different modes of normalization were each corrected downward to compensate for the accidental appearance of an L -counter signal in coincidence with a real 2γ event. This correction was determined experimentally to be approximately 15% by noting the number of L -counter coincidences when all six γ 's from a $3\pi^0$ event are visible and by noting the number of times an L counter is accidentally activated on a $\pi e\nu$ or $\pi\mu\nu$ decay. After this correction we obtained the following results:

$$\begin{aligned} \text{No. of } K_L^0 \text{ decays as derived from } 3\pi^0 \text{ events} \\ = (387 \pm 21) \times 10^3; \end{aligned}$$

$$\begin{aligned} \text{No. of } K_L^0 \text{ decays as derived from } \pi\mu\nu \text{ events} \\ = (417 \pm 28) \times 10^3; \end{aligned}$$

$$\begin{aligned} \text{No. of } K_L^0 \text{ decays as derived from } \pi e\nu \text{ events} \\ = (383 \pm 35) \times 10^3. \end{aligned}$$

It is clear that these results are quite consistent with each other. The over-all result is

$$\text{No. of } K_L^0 \text{ decays} = (396 \pm 16) \times 10^3.$$

All film used in the normalization calculation was also scanned for possible 2γ candidates. The basic criteria for a picture to be listed as a 2γ event was that two and only two γ showers be visible in the chamber. All these events were then rescanned and checks were made using the counter data. In order not to be eliminated from further considerations, each of the rescanned candidates had to have at least one γ which started at the front of the chamber and extrapolated back to a valid trigger-counter triplet, and also the second γ had to be directed in such a way as to not obviously violate momentum conservation, assuming that the γ 's had originated from a K_L^0 coming down the beam line. This meant that the γ had to be in opposite quadrants of the vertical plane of the spark chamber. Also eliminated in the rescan were those events where the S counters indicated that an extra γ had passed through the chamber hole.

The 273 events remaining after the rescan were divided into two classes, 140 with no L counters and 133 with one or more L counters. Ideally, for a genuine 2γ decay, no L 's should count if the two γ 's go into the chamber. But, as was seen with the 6γ events, a certain fraction of genuine 2γ de-

cays could have counted in the L 's accidentally. Following our criteria for the calculation of the normalization, we have used only those events without L counts for the calculation of the number of genuine 2γ events.

Using the measured direction cosines, the two γ 's were fitted to the hypothesis $K_L^0 \rightarrow 2\gamma$ by using two straight lines, originating from a common vertex which was within the constraints of the collimator. The quantity upon which we based the selection of our valid 2γ events is the collinearity of the decay in the K_L^0 center-of-mass frame. The collinearity is defined as $\cos\theta_{\gamma_1\gamma_2}^{\text{c.m.}}$, the cosine of the opening angle between the two γ rays after they have been transformed to the kaon center-of-mass frame, as determined by the measured time of flight. After our events were selected, we studied several other associated quantities to verify the hypothesis of $K_L^0 \rightarrow 2\gamma$.

Of the 140 events with no L count, 38 had a first measurement giving $\cos\theta_{\gamma_1\gamma_2}^{\text{c.m.}} < -0.90$. These events were remeasured a second time and approximately 15% of the events showed a clear measurement error. The mismeasured events were remeasured a third time and the bad measurement was eliminated by comparison with the other two. In Fig. 6 we have plotted the first good measurement of $\cos\theta_{\gamma_1\gamma_2}^{\text{c.m.}}$ for all events in the region $\cos\theta_{\gamma_1\gamma_2}^{\text{c.m.}} < -0.50$. For comparison in Fig. 7 we have plotted all of the events with L counts. The absence of a peak at $\cos\theta_{\gamma_1\gamma_2}^{\text{c.m.}} = -1$ among the events with counts in the L counters and the presence of a peak at $\cos\theta_{\gamma_1\gamma_2}^{\text{c.m.}} = -1$ among the events without L counts attests to the fact that we are indeed observing real 2γ events.

In order to determine the total number of genu-

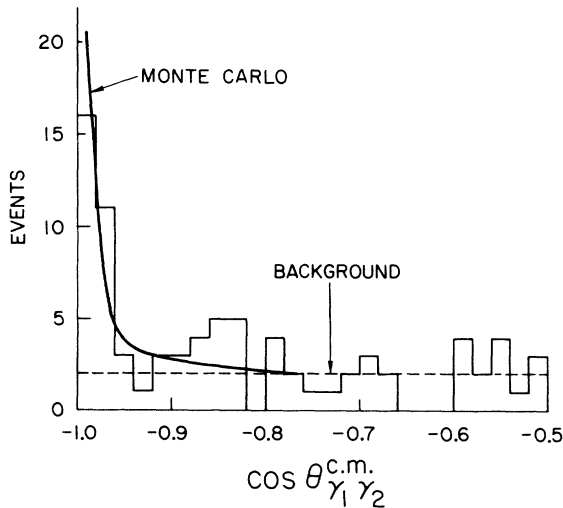


FIG. 6. Collinearity distribution for all unlatched 2γ events.

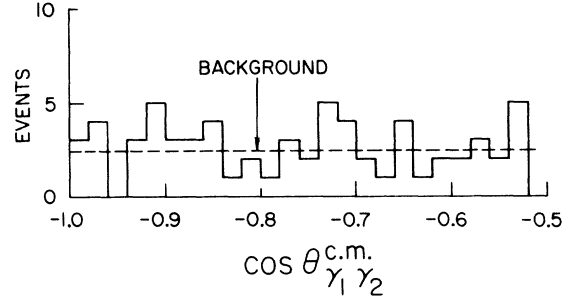


FIG. 7. Collinearity distribution for all latched 2γ events.

ine 2γ events over all values of $\cos\theta_{\gamma_1\gamma_2}^{\text{c.m.}}$, we must understand the measurement and timing errors that were present in the reconstruction and transformation to the center-of-mass system. The measuring error originated from two independent sources. The first error was due to the Coulomb scattering of the shower particles in the chamber. Since the electron and positron both scatter independently about the initial photon direction the average deviation is

$$\langle\theta^2\rangle = \frac{1}{2}\langle\theta_e^2\rangle$$

or

$$\overline{\Delta\theta_{\text{scat}}} = \sqrt{\langle\theta^2\rangle} = \frac{1}{\sqrt{2}} \frac{21}{P_e} = \frac{15 \text{ MeV}}{P_e} \approx \frac{25 \text{ MeV}}{E_\gamma},$$

assuming $P_e \approx \frac{1}{2}P_\gamma = \frac{1}{2}E_\gamma$. The second error was the error which occurred in actually measuring the best line which represented the shower direction. This error was estimated by comparing the two measurements of all the good 2γ events, yielding

$$\overline{\Delta\theta_{\text{meas}}} \approx 0.025 \text{ rad.}$$

Note that we have not included any angular error which might be due to possible systematic effects such as local distortions in the Lucite, rotation of

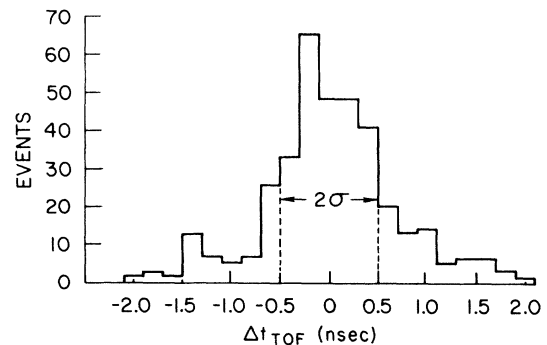


FIG. 8. Difference between corrected triplet times for good $3-6\gamma$ events from first data run.

TABLE I. Summary of $K_L^0 \rightarrow 2\gamma$ measurements.

Date	Group	Method	Normalization	Total 2γ events	Branching ratio, $BR_{\gamma\gamma}$	Reference
1967	Princeton (1)	Spark-chamber spectrometer	$3\pi^0$	90	$(5.5 \pm 1.1) \times 10^{-4}$	1
1967	Illinois	Spark-chamber shower counter	$\pi\mu\nu_\mu, \pi e\nu_e, \pi^+\pi^-\pi^0$	32	$(6.7 \pm 2.2) \times 10^{-4}$	2
1968	Princeton (2)	Spark-chamber spectrometer	$3\pi^0$	115	$(4.7 \pm 0.6) \times 10^{-4}$	3
1968	CERN-Orsay	Heavy-liquid bubble chamber	$3\pi^0$	16	$(5.3 \pm 1.5) \times 10^{-4}$	4
1970	Particle Data Group	Weighted average			$(5.2 \pm 0.5) \times 10^{-4}$	19
1971	Stanford	Spark-chamber shower counter	$3\pi^0, \pi\mu\nu_\mu, \pi e\nu_e$	23	$(4.5 \pm 1.0) \times 10^{-4}$	

the chamber, and so forth, because we estimated these would result in an error small compared to the intrinsic measuring error discussed above.

The other error which was present was the time-of-flight error caused by statistical fluctuations in the measured counter times. We took a sample of events in which two independent γ 's were observed in the front counters (T and F) and plotted the difference between the two independently determined times of flight (TOF). Such a plot, shown in Fig. 8, indicates a standard deviation of

$$\overline{\Delta t}_{\text{TOF}} = 0.5 \pm 0.1 \text{ nsec.}$$

Assuming normal errors, this leads to a time resolution in each case of

$$\overline{\delta t}_{\text{TOF}} = \overline{\Delta t}_{\text{TOF}} / \sqrt{2} = 0.35 \pm 0.07 \text{ nsec} \approx 0.4 \text{ nsec.}$$

The timing and measurement errors determined above were then used in the Monte Carlo calculator to obtain the time rate of $K_L^0 \rightarrow 2\gamma$ decays subject to a background level determined empirically. The result of this calculation is superimposed on the experimental data of Fig. 6 and fits well. Making a cut at $\cos\theta_{\gamma_1\gamma_2}^{\text{c.m.}} < -0.96$ we are left with 27 ± 5 events. Subtracting a background of 4 ± 1 events, we have

$$N_{\gamma\gamma} = 23 \pm 5.$$

The fraction of Monte Carlo 2γ events satisfying this $\cos\theta$ cut is 0.80 ± 0.04 . The average efficiency for observing *both* γ 's in the chamber and giving the proper trigger is 0.163 ± 0.010 . This leads us to a branching ratio of

$$BR_{\gamma\gamma} = \frac{(23 \pm 5)/(0.80 \pm 0.04)(0.163 \pm 0.01)}{396\,000 \pm 16\,000} \\ = 4.5 \pm 1.0 \times 10^{-4}.$$

IV. CONCLUSIONS

The branching ratio which we have obtained of $BR_{\gamma\gamma} = (4.5 \pm 1.0) \times 10^{-4}$ is consistent with the other determinations of this number, which are summarized in Table I, and with the currently accepted weighted average of¹⁹

$$BR_{\gamma\gamma} = (5.2 \pm 0.5) \times 10^{-4}.$$

We believe the experimental method employed here for measuring this decay mode is intrinsically straightforward and free of any systematic effects which could possibly cause a large error in the answer. The main limitation on the accuracy of the result is at present statistical.

ACKNOWLEDGMENTS

The successful completion of this experiment depended upon the valuable support received from several quarters. We are indebted to Karl Hense, Dale Ouimette, and Don Clark for building and maintaining much of the equipment used in the experiment. George Ike and Jeff Hobson are to be thanked for measuring the spark-chamber film. Needless to say, none of this work could have been carried out without the complete support of the Stanford Linear Accelerator Center.

*Work supported in part by the U. S. Atomic Energy Commission and the U. S. Air Force Office of Scientific

Research under Contract No. F44620-67-C-0070.
†Present address: Weizmann Institute of Science,

Rehovoth, Israel.

‡Present address: University of California, Santa Cruz, California; Alfred P. Sloan Foundation Fellow.

§Present address: University of Hawaii, Hilo, Hawaii.

||Present address: Cambridge University, Cambridge, England.

**Alfred P. Sloan Foundation Fellow.

¹J. Cronin, P. Kunz, W. Risk, and P. Wheeler, *Phys. Rev. Letters* **18**, 25 (1967); P. Kunz, thesis, Princeton University, 1968 [Elementary Particles Laboratory Report No. 46 (unpublished)].

²J. Todoroff, thesis, University of Illinois, 1967 (unpublished).

³M. Banner, J. W. Cronin, J. K. Liu, and J. E. Pilcher, *Phys. Rev. Letters* **21**, 1107 (1968). J. Pilcher, thesis, Princeton University, 1968 [Elementary Particles Laboratory Report No. 49 (unpublished)].

⁴R. Arnold, I. A. Budagov, D. C. Cundy, G. Myatt, F. Nezzrick, G. H. Trilling, W. Venus, H. Yoshiki, B. Aubert, P. Heusse, E. Nagy, and C. Pascaud, *Phys. Letters* **28B**, 56 (1968).

⁵M. Banner, J. W. Cronin, J. K. Liu, and J. E. Pilcher, *Phys. Rev.* **188**, 2033 (1969).

⁶J. Dreitlein and H. Primakoff, *Phys. Rev.* **124**, 268 (1961).

⁷S. Oneda and S. Hori, *Phys. Rev.* **132**, 1800 (1963).

⁸C. Bouchiat, J. Nuyts, and J. Prentki, *Phys. Letters* **3**, 156 (1963).

⁹S. Oneda, Y. S. Kim, and D. Korff, *Phys. Rev.* **136B**,

1064 (1964).

¹⁰V. K. Ignatovich and B. V. Struminsky, *Phys. Letters* **24B**, 69 (1967).

¹¹L. M. Sehgal and L. Wolfenstein, *Phys. Rev.* **162**, 1362 (1967).

¹²H. Stern, *Nuovo Cimento* **51A**, 195 (1967).

¹³S. Oneda and J. Pati, *Phys. Rev.* **155**, 1621 (1967).

¹⁴D. F. Greenberg, *Nuovo Cimento* **56A**, 597 (1968).

¹⁵C. A. Savoy and A. H. Zimmerman, *Nuovo Cimento* **57A**, 201 (1968).

¹⁶B. R. Martin and E. de Rafael, *Nucl. Phys.* **B8**, 131 (1968).

¹⁷R. Rockmore, *Phys. Rev.* **182**, 1512 (1969); **187**, 2125 (1969).

¹⁸N. N. Wong, *Phys. Rev. D* **2**, 625 (1970).

¹⁹Particle Data Group, *Phys. Letters* **33B**, 1 (1970).

²⁰R. B. Neal, *The Stanford Two-Mile Accelerator* (Benjamin, New York, 1968).

²¹A. D. Brody, W. B. Johnson, D. W. G. S. Leith, G. Loew, J. S. Loos, G. Luste, R. Miller, K. Moriyasu, B. C. Shen, W. M. Smart, and R. Yamartino, *Phys. Rev. Letters* **22**, 966 (1969).

²²A detailed description of the experiment can be found in J. E. Enstrom, thesis, Stanford University, 1970 [SLAC Report No. SLAC-125 (unpublished)].

²³D. Porat and K. Hense, *Nucl. Instr. Methods* **67**, 229 (1969).

²⁴S. W. MacDowell, *Nuovo Cimento* **6**, 1445 (1957).

K^+p Elastic Scattering Between 432 and 939 MeV/c

C. J. Adams,* J. D. Davies, J. D. Dowell, G. H. Grayer,† P. M. Hattersley,† R. J. Howells,‡
C. McLeod, T. J. McMahon, H. B. van der Raay, and L. Rob§
Birmingham University, Birmingham, England

and

C. J. S. Damerell, R. J. Homer, and M. J. Hotchkiss
Rutherford High Energy Laboratory, Chilton, Berkshire, England
(Received 17 June 1971)

We present data from a spark-chamber study of K^+p elastic scattering between 432 and 939 MeV/c, over the range $-0.6 < \cos\theta_{c.m.} < +0.7$. With measurements at 13 momenta, and between 2000 events at the lowest momentum and 5000 events at the highest momentum, there is a major improvement over previous data. The elastic cross sections deduced from the differential cross sections are almost independent of momentum through the range covered. The data are inconsistent with counter measurements of the total cross section which suggest a sharp shoulder in the cross section at about 700 MeV/c.

In this paper, we present data on low-momentum K^+p elastic scattering obtained in a spark-chamber experiment at the Rutherford Laboratory 7-GeV proton synchrotron. The low-momentum region for K^+p elastic scattering has recently been the subject of renewed interest from the viewpoint of phase-shift analysis. The traditional assumption

of dominant S wave with negative phase shift has been questioned.¹ Improved data on small-angle K^+p scattering at low momenta are needed to clarify this situation. Experimental evidence that the low-momentum K^+p scattering is not smoothly varying has been obtained in counter measurements of the total cross section. The earlier re-